reveals an effective C_3 point group about terbium rather than D_{3h}, D_3, or C_{3h} symmetry. The spectra do not appreciably change in CH_2Cl_2 and toluene solvents. An interpretation of these results is that, in the crystalline form and in solutions of noncoordinating solvents, the three three-center, bridging BH---Tb interactions influence the luminescence spectra of **2**. In donor solvents, complexation of $[H_2B(pz)_2]_3Tb$ with the solvent molecules changes the lifetime and the spectral features of the luminescence. For these cases, coordination of the solvent results in a change in the coordination environment about terbium.

Contribution from the Department of Chemistry,
York University, North York (Toronto), Ontario, Canada M3J 1P3

Control of Orbital Mixing in Ruthenium Complexes Containing Quinone-Related Ligands

Hitoshi Masui, A. B. P. Lever,* and Pamela R. Auburn

Received August 14, 1990

Three redox series of complexes of the general formulas $Ru^{II}(bpy)_2LL$ and $Ru^{II}(py)_4LL$ (bpy = 2,2'-bipyridine) are reported, where LL are the ligands 1,2-dihydroxybenzene, 2-aminophenol, and 1,2-diaminobenzene. These ligands can exist in the fully reduced catechol form or the one and two electron oxidized semiquinone and quinone forms. Electronic and electron spin resonance spectroscopic and electrochemical data are discussed in terms of orbital mixing and electronic structure and the number of oxygen or nitrogen atoms in the coordinating ligand.

Introduction

There has been considerable interest in the study of transition-metal complexes of noninnocent, quinone-related ligands including those of dithiolenes,[1-3] dioxolenes,[4-16] and benzoquinonediimines.[17-33] The possibility of electron delocalization between the metal and the ligand has been a major theme in the study of these systems.[30,34-36] The electron distribution will depend on the extent of mixing between the metal and ligand orbitals, which, in turn, is a function of the energies, symmetries, and overlap of the valence metal and ligand orbitals.

Previous studies of ruthenium dioxolene complexes (dioxolene = catechol, semiquinone, quinone)[7-9] have found unusually large

Scheme I. *o*-Phenylene Ligand Redox Isomers[a]

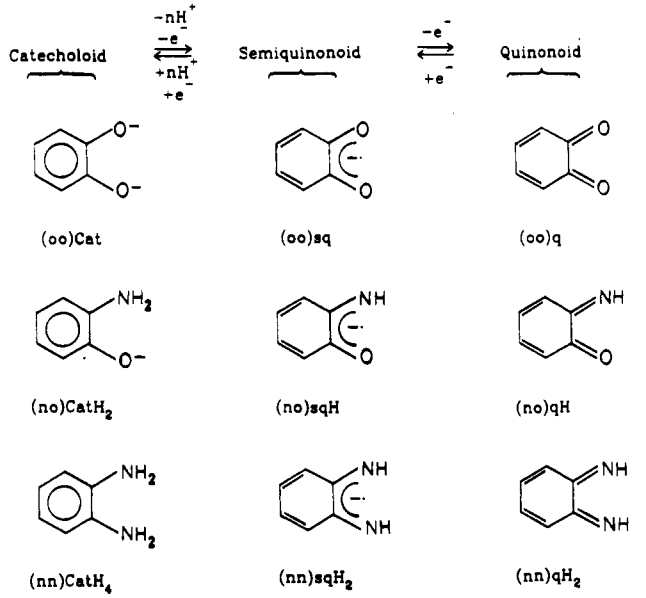

[a] Key: for (nn), $n = 2$; for (no), $n = 1$; for (oo), $n = 0$.

(1) Burns, R. P.; McAuliffe, C. A. *Adv. Inorg. Chem. Radiochem.* **1979**, *22*, 303.
(2) Eisenberg, R. *Prog. Inorg. Chem.* **1970**, *12*, 295.
(3) McCleverty, J. A. *Prog. Inorg. Chem.* **1968**, *10*, 49.
(4) Kessel, S. L.; Emerson, R. M.; Debrunner, P. G.; Hendrickson, D. N. *Inorg. Chem.* **1980**, *19*, 1170.
(5) Buchanan, R. M.; Claflin, J.; Pierpont, C. G. *Inorg. Chem.* **1983**, *22*, 2552.
(6) Harmalker, S.; Jones, S. E.; Sawyer, D. T. *Inorg. Chem.* **1983**, *22*, 2790.
(7) Haga, M.-A.; Dodsworth, E. S.; Lever, A. B. P. *Inorg. Chem.* **1986**, *25*, 447.
(8) Stufkens, D. J.; Snoeck, Th. L.; Lever, A. B. P. *Inorg. Chem.* **1988**, *27*, 935.
(9) Lever, A. B. P.; Auburn, P. R.; Dodsworth, E. S.; Haga, M.-A.; Liu, W.; Melnik, M.; Nevin, W. A. *J. Am. Chem. Soc.* **1988**, *110*, 8076.
(10) Thompson, J. S.; Calabrese, J. C. *Inorg. Chem.* **1985**, *24*, 3167.
(11) Sofen, S. R.; Ware, D. C.; Cooper, S. R.; Raymond, K. N. *Inorg. Chem.* **1979**, *18*, 234.
(12) Boone, S. R.; Pierpont, C. G. *Inorg. Chem.* **1987**, *26*, 1769.
(13) Espinet, P.; Bailey, P. M.; Maitlis, P. M. *J. Chem. Soc., Dalton Trans.* **1979**, 1542.
(14) Pierpont, C. G.; Buchanan, R. M. *Coord. Chem. Rev.* **1981**, *38*, 45.
(15) Cooper, S. R.; Koh, Y. B.; Raymond, K. N. *J. Am. Chem. Soc.* **1982**, *102*, 5092.
(16) Benelli, C.; Dei, A.; Gatteschi, D.; Pardi, L. *Inorg. Chem.* **1989**, *28*, 1476.
(17) Balch, A. L.; Holm, R. H. *J. Am. Chem. Soc.* **1966**, *88*, 5201.
(18) Baikie, P. E.; Mills, O. S. *Inorg. Chim. Acta* **1967**, *1*, 55.
(19) Duff, E. J. *J. Chem. Soc. A* **1968**, 434.
(20) Warren, L. F. *Inorg. Chem.* **1977**, *16*, 2814.
(21) Reinhold, J.; Benedix, R.; Birner, P.; Hennig, H. *Inorg. Chim. Acta* **1979**, *33*, 209.
(22) Vogler, A.; Kunkely, H. *Angew. Chem., Int. Ed. Engl.* **1980**, *19*, 221.
(23) Belser, P.; von Zelewsky, A.; Zehnder, M. *Inorg. Chem.* **1981**, *20*, 3098.
(24) El'Cov, A. V.; Maslennikova, T. A.; Kukuschkin, V. Ju.; Shavurov, V. V. *J. Prakt. Chem.* **1983**, *B325*, S27.
(25) Pyle, A. M.; Barton, J. K. *Inorg. Chem.* **1987**, *26*, 3820.
(26) Thorn, D. L.; Hoffmann, R. *Nouv. J. Chim.* **1979**, *3*, 39.
(27) Peng, S.-M.; Chen, C.-T.; Liaw, D.-S.; Chen, C.-I.; Wang, Y. *Inorg. Chim. Acta* **1985**, *101*, L31.
(28) Christoph, G. G.; Goedken, V. L. *J. Am. Chem. Soc.* **1973**, *95*, 3869.
(29) Hall, G. S.; Soderberg, R. H. *Inorg. Chem.* **1968**, *7*, 2300.
(30) Gross, M. E.; Ibers, J. A.; Trogler, W. C. *Organometallics* **1982**, *1*, 530.
(31) Zehnder, M.; Loliger, H. *Helv. Chim. Acta* **1980**, *63*, 754.
(32) Danopoulos, A. A.; Wong, A. C. C.; Wilkinson, G.; Hursthouse, M. B.; Hussain, B. *J. Chem. Soc., Dalton Trans.* **1990**, 315.
(33) Nemeth, S.; Simandi, L. I.; Argay, G.; Kalaman, A. *Inorg. Chim. Acta* **1989**, *166*.
(34) Gross, M. E.; Trogler, W. C.; Ibers, J. A. *J. Am. Chem. Soc.* **1981**, *103*, 192.
(35) Miller, E. J.; Brill, T. B. *Inorg. Chem.* **1983**, *22*, 2392.
(36) Miller, E. J.; Landon, S. J.; Brill, T. B. *Organometallics* **1985**, *4*, 533.

0020-1669/91/1330-2402$02.50/0

degrees of orbital mixing between the metal and the ligand. The successive substitution of the dioxolene oxygen atoms with less electronegative nitrogen atoms may be expected to change this mixing in a systematic fashion depending upon ligand charge and oxidation state.

To investigate the effects of such variations, a series of ruthenium complexes were synthesized containing *o*-phenylene ligands (Scheme I). The *o*-phenylene ligands, which include catechols, (oo), *o*-aminophenols, (no), and *o*-phenylenediamines, (nn), have three easily accessed redox forms: the fully reduced catechol form, $catH_n$, the partially oxidized semiquinone form, sqH_n, and the fully oxidized quinone form, qH_n, which can exist in various states of protonation. The subscript, *n*, reflects the number of protons attached to the donor atoms in each species (Scheme I).

The synthesis of three compounds by successive replacement of the oxygen atoms by nitrogen yields, through permutation of the three oxidation states, nine species whose orbital energies can be probed via their rich electronic spectra. These *o*-phenylene ligands form fairly stable semiquinone complexes whose electron spin resonance (ESR) spectra may also be used to estimate the degree of orbital mixing within the complexes.

Reported here are the synthesis and characterization by electrochemistry, electronic spectroscopy, photoelectron spectroscopy, and ESR spectroscopy of the mixed-ligand redox series $[RuN_4LL]^{n+}$, where N_4 = bis(2,2′-bipyridine) (bpy) or tetrapyridine (py) and LL = *o*-phenylene ligand.

Specific abbreviations for complexes are shown in the Experimental Section. Thus, bpy(nn)qH_2 refers to the (bipyridine)ruthenium(II) complex containing the *o*-phenylenediamine ligand in its quinone oxidation state, while (no)$catH_2$ would refer to complexes of the aminophenol ligand, in its catechol oxidation state, where no distinction is drawn between pyridine- or bipyridine-bound ruthenium. The labels (oo), (no), and (nn) will be used to designate complexes of these *o*-phenylene ligands where no distinctions are made between the pyridine- and bipyridine-bound species or between oxidation states.

Our spectroscopic data for bpy(nn)qH_2 agree with data in a previous report.[23] We differ, however, in reporting reversible or quasi-reversible electrochemistry for this species, which had previously been reported to display highly irreversible electrochemistry.

Experimental Section

Reagents. All solvents and reagents used for synthetic purposes were reagent grade or better and used as purchased except where otherwise stated. *o*-Phenylenediamine (BDH) was recrystallized from benzene, and cobaltocene (Strem) was sublimed, before use. Aldrich Gold Label acetonitrile (MeCN), BDH dichloroethane (DCE), and Aldrich 2-methyl-tetrahydrofuran (MeTHF) were distilled from P_2O_5, CaH_2, and sodium, respectively. Tetrabutylammonium perchlorate (TBAP) and tetrabutylammonium hexafluorophosphate (Kodak; TBAH) were recrystallized from absolute ethanol and dried under vacuum at 100 °C for 24 h. Benzoyl peroxide (BDH) was dried at 100 °C for 24 h before use.

Physical Measurements. Spectroscopic measurements were recorded on the following instruments: UV/vis spectra, Hitachi Perkin-Elmer Model 340 microprocessor spectrophotometer or a Varian Cary 2400 spectrophotometer; ESR spectra, Varian E4 electron spin resonance spectrophotometer (X-band; 77 K in frozen solutions of DCE or MeTHF). Photoelectron (PES) data were recorded in the Surface Science Laboratory of the University of Western Ontario. Binding energies are relative to C(1s) at 285.0 eV with an estimated error of ±0.3 eV.

Cyclic voltammetry (CV) was performed in 0.1 M TBAP or TBAH solutions in either DCE or acetonitrile on Princeton Applied Research Models 173, 174, and 175 instrumentation. Platinum wires served as counter and working electrodes against a nonaqueous AgCl/Ag (−0.037 V vs SCE) reference electrode. The potentials are reported vs SCE.

Bulk electrolysis and spectroelectrochemistry were performed in a 1-cm glass cuvette by using a platinum-gauze working electrode, nichrome-wire counter electrode (separated from solution by a frit), and a nonaqueous AgCl/Ag reference electrode. Nitrogen gas, saturated with solvent, was continuously bubbled through the cell to provide both mixing and an inert atmosphere.

All syntheses were performed under nitrogen except where otherwise stated. The CHN microanalyses were performed by the Canadian Microanalytical Service, Vancouver, Canada.

Preparation of Complexes. **$[Ru(bpy)_2(nn)catH_4](PF_6)_2$ = bpy(nn)$catH_4$.** A mixture containing ethanol (6 mL), anhydrous $Ru(bpy)_2Cl_2$[37] (0.102 g, 0.22 mmol), and *o*-phenylenediamine (0.025 g, 0.23 mmol) was refluxed for 4 h, during which time a red solution formed. The solution was cooled to room temperature and acidified with 1:10 acetic acid/ethanol (0.2 mL). A solution of NH_4PF_6 (0.3 g) in water (10 mL) was added to the solution. The mixture was boiled until all of the resulting precipitate dissolved. The solution was cooled slowly to room temperature, during which time orange-red crystals formed. The crystals were isolated by filtration in air, washed with 2% acetic acid, copious amounts of ether, and hexanes, and air-dried. Yield: 0.14 g, 81%. PES (Ru $3d_{5/2}$): 280.8 eV. Anal. Calcd for $C_{26}H_{24}F_{12}N_6P_2Ru$: C, 38.48; H, 2.98; N, 10.36. Found: C, 38.29; H, 2.92; N, 10.20.

$[Ru(bpy)_2(nn)sqH_2](PF_6)$ = bpy(nn)sqH_2. For spectroscopic purposes, this material was prepared by the addition of an excess of bpy(nn)qH_2 to a dilute solution of cobaltocene in MeTHF. The resulting blue solution, which contains the PF_6^- salts of the desired complex and the cobaltocenium ion, was decanted from the unreacted bpy(nn)qH_2, which remained insoluble in MeTHF. The product showed electronic and ESR spectra that were identical with those obtained by the electrochemical reduction of bpy(nn)qH_2 at a potential slightly negative of the first reduction wave. The compound was not isolated because of its reactivity toward oxygen and water. The cobaltocenium ion present in the reaction mixture did not significantly interfere with the electronic spectrum because of its relatively low extinction coefficient below 25 000 cm^{-1} (<100 L mol^{-1} cm^{-1}).

$[Ru(bpy)_2(nn)qH_2](PF_6)_2$ = bpy(nn)qH_2. This compound was synthesized by using a modified procedure of von Zelewsky[23] as follows. A saturated solution of bpy(nn)$catH_4$ in concentrated ammonia/acetone/water (1:5:4) was bubbled with air for 3.5 h, during which time the red color deepened. The solution was flash evaporated to dryness, and the residue was redissolved in a minimum amount of boiling water to which was added 10 equiv of NH_4PF_6. Subsequent slow cooling to room temperature gave copper-colored crystals of product, which were isolated by filtration, rinsed with sparing amounts of cold water followed by copious amounts of ether and hexanes, and air-dried. Yield: >80%. PES (Ru $3d_{5/2}$): 281.4 eV. Anal. Calcd for $C_{26}H_{22}F_{12}N_6P_2Ru$: C, 38.57; H, 2.77; N, 10.38. Found: C, 38.78; H, 2.90; N, 10.10.

$[Ru(py)_4(nn)qH_2](PF_6)_2$ = py(nn)qH_2. Silver nitrate (0.070 g, 0.41 mmol) was added to a suspension of *trans*-$Ru(py)_4Cl_2$[38] (0.10 g, 0.21 mmol) in methanol. Stirring was maintained for 30 min, after which the precipitated AgCl was removed by filtration through Celite. To the filtrate was added solid *o*-phenylenediamine (0.022 g, 0.21 mmol), and after being stirred for 30 min, the orange solution was bubbled with air for 1 h, during which time the solution became purple. A 1% solution of NH_4PF_6 (10 mL) was added to the solution, which was subsequently concentrated until the product began to precipitate. The product was redissolved by heating and reprecipitated by slow cooling to −15 °C. The resulting crude product was isolated by filtration and purified by Soxhlet extraction with DCE. Crystals were obtained by slowly diffusing diethyl ether into the extract. Yield: 50%. Anal. Calcd for $C_{26}H_{26}F_{12}N_6P_2Ru$: C, 38.38; H, 3.22; N, 10.83. Found: C, 37.71; H, 3.39; N, 10.01.

$[Ru(py)_4(nn)sqH_2](PF_6)$ = py(nn)sqH_2. For spectroscopic purposes, blue-green solutions of this compound were chemically generated in the same manner as bpy(nn)sqH_2. However, it was harder to generate this compound electrochemically than the bipyridine analogue, since a steady-state current was approached, indicating that the solvent (DCE or acetonitrile) was catalytically reduced by the compound.

$[Ru(py)_4(nn)catH_4](PF_6)_2$ = py(nn)$catH_4$. For spectroscopic purposes, yellow solutions of this compound were generated by reducing py(nn)qH_2 with zinc amalgam in 10% aqueous acetic acid solutions or by bulk electrolysis in the same medium at −0.36 V vs SCE. The product gave the same electronic spectrum as the reaction mixture used to prepare py(nn)qH_2 but prior to air oxidation. This complex oxidizes in air at a moderate rate.

$[Ru(bpy)_2(no)catH_2](ClO_4)$ = bpy(no)$catH_2$. To a suspension of $Ru(bpy)_2Cl_2$ (0.1 g, 0.21 mmol) in methanol (5 mL) was added silver nitrate (0.069 g, 0.21 mmol) in methanol (5 mL). After 30 min of stirring, the precipitated AgCl was removed by filtration through Celite. Methanolic triethylamine (10%, 0.21 mmol, 0.29 mL) followed by 2-aminophenol (0.025 g, 0.23 mmol) in methanol (5 mL) was added dropwise to the filtrate while the solution was stirring. The resulting blood red solution was refluxed for 30 min and then reduced in volume to 5 mL by passing N_2 over the hot solution. Lithium perchlorate trihydrate (0.036 g, 0.23 mmol) in methanol (2 mL) was added to the hot reaction mixture. The

(37) Sullivan, B. P.; Salmon, D. J.; Meyer, T. J. *Inorg. Chem.* **1978**, *17*, 3334.
(38) Evans, I. P.; Spencer, A.; Wilkinson, G. *J. Chem. Soc., Dalton Trans.* **1973**, 204.

mixture was cooled to room temperature and toluene/diethyl ether (2:1, 65 mL) was gently added to the quiescent solution. The mixture was allowed to sit overnight, during which time cubic, black crystals were deposited. The product was collected by filtration and washed with copious amounts of toluene and hexanes. Yield: >80%. Anal. Calcd for $C_{26}H_{22}ClN_5O_5Ru$: C, 50.28; H, 3.57; N, 11.28. Found: C, 52.15; H, 3.84; N, 11.96.

$[Ru(bpy)_2(no)sqH]^+$ = bpy(no)sqH and $[Ru(bpy)_2(no)qH]^{2+}$ = bpy(no)qH. These species were generated from dilute DCE solutions of $[Ru(bpy)_2(no)catH_2](ClO_4)$ by the stoichiometric addition of benzoyl peroxide. The semiquinone complex is brown in solution, while the quinone complex is purple. Although these species were not isolated, the reactions were reversible by the addition of methanolic ascorbic acid solutions, indicating that the oxidation processes did not decompose the complexes.

$Ru(bpy)_2(oo)cat$ = bpy(oo)cat. The synthesis of this compound and its redox isomers is described elsewhere.[7,8]

$[Ru(py)_4(oo)sq](PF_6)$ = py(oo)sq. To a stirred mixture of *trans*-$Ru(py)_4Cl_2$ (0.1 g, 0.21 mmol) and catechol (0.023 g, 0.205 mmol) in deoxygenated methanol (30 mL) was added a methanolic solution of sodium hydroxide (2 mL, 0.2 M). This mixture was refluxed for 16 h, during which time the $Ru(py)_4Cl_2$ dissolved, giving, initially, a blood red solution and then a brown solution. The solution was exposed to air, filtered, and allowed to cool. During this process, the color of the solution changed to green. After this solution cooled to room temperature, a solution of NH_4PF_6 (0.1 g) in water (2 mL) was added. The solution was allowed to stand at room temperature for 5 days, thereby yielding dark green crystals of py(oo)sq·$2H_2O$ (0.52 g, 36%). These were collected by filtration, washed with 2:1 methanol/water and diethyl ether, and air-dried. Anal. Calcd for $C_{26}H_{28}F_6N_4O_4PRu$: C, 44.19; H, 3.99; N, 7.93. Found: C, 44.09; H, 3.48; N, 8.25.

$Ru(py)_4(oo)cat$ = py(oo)cat and $Ru(py)_4(oo)q(PF_6)_2$ = py(oo)q. These compounds were easily obtained by bulk electrolysis in DCE solutions of py(oo)sq, at −0.4 and 0.8 V vs SCE, respectively. The reduced species is bright yellow in dilute solutions, while the oxidized species is green-blue.

Attempted Syntheses. $[Ru(py)_4(no)catH_2](PF_6)$ = py(no)$catH_2$. Attempts to synthesize this compound by procedures similar to those used in the other *o*-phenylene ligand complexes produced a yellow, unidentified compound. Thus, the redox series of this complex could not be obtained.

Deprotonated Species. Attempts were also made to characterize deprotonated forms of the bpy(nn) and (no) catechol complexes to maintain constant the number of protons within each *o*-phenylene ligand group. Such deprotonated species are stable in high-oxidation-state rhenium and osmium complexes;[32] however, we were quite unable to obtain these species in our ruthenium(II) series either by electrochemical or chemical methods. Electrochemical polarization slightly negative of the second reduction couple of bpy(nn)qH_2 in aprotic media generated what appeared to be a mixture of bpy(nn)sqH_2 and bpy(nn)$catH_4$. The current reached a steady state due to catalytic solvent reduction. Removal of the applied potential from the cell caused the majority of species in solution to be rapidly oxidized to bpy(nn)sqH_2, regardless of the inert atmosphere.

Attempts to chemically reduce bpy(nn)qH_2 by two electrons using sodium amalgam in propylene carbonate solution initially generated bpy(nn)sqH_2, after which a yellow decomposition product irreversibly formed. Deprotonation of bpy(nn)$catH_4$ using several strong bases, including sodium methoxide in methanol solution, sodium amide suspension in pyridine, and lithium aluminum hydride suspension in THF (this required the use of the 4,5-dimethylated *o*-phenylenediamine complex for solubility reasons), initially formed what was determined by electronic and ESR spectroscopy to be bpy(nn)sqH_2. The latter two reactions further produced a species whose electronic spectrum resembled that of bpy(nn)qH_2. Since all of the color changes developed at the interface between the solution and the particles of base, leakage of oxygen into the air-sensitive system could be ruled out as a cause of the apparent oxidations.

Results and Discussion

Electrochemistry. The cyclic voltammograms of the *o*-phenylene ligand complexes show multiple couples, which result from redox processes centered at the metal, the *o*-phenylene ligand, and the bpy ligands. Using arguments discussed previously,[7] one may assign these couples as shown in Table I.

With the exception of bpy(nn)$catH_4$ and bpy(no)$catH_2$, the cyclic voltammograms of the *o*-phenylene complexes, in an organic solvent, show two chemically reversible *o*-phenylene ligand couples that shift negatively as oxygen donors are replaced by the more electron-rich nitrogen atoms on the *o*-phenylene ligand (Table I and Figure 1). The bpy(nn)$catH_4$ and bpy(no)$catH_2$ complexes show a chemically irreversible two-electron oxidation wave attributed to the concomitant, irreversible loss of a hydrogen atom from each *o*-phenylene ligand nitrogen atom during the oxidation of the ligand from the catechol to quinone form (Figure 2).

Table I. Electrochemical Potentials (V) of RuN_4L Complexes, Where N_4 = Bis(bipyridine)/Tetrapyridine and L = *o*-Phenylene Ligand[a]

species	Ru(III)/Ru(II)	L/L^{2-}	bpy/bpy⁻(1)	bpy/bpy⁻(2)
bpy(nn)$catH_4$	1.37[b]	0.99[b,c]	−1.58[d]	−1.83[b,c]
bpy(no)$catH_2$	1.48[b]	0.34[b,c]	−1.56[b]	−1.80[b]

species	Ru(III)/Ru(II)	L/L^-	L^-/L^{2-}	bpy/bpy⁻(1)	bpy/bpy⁻(2)
bpy(oo)q[e]	1.65[b]	0.56	−0.33	−1.72	
py(oo)q	1.52[b]	0.59	−0.34		
bpy(nn)qH_2	1.35	−0.47	−1.15[d]	−1.72[d]	−1.96[d]
py(nn)qH_2	1.33[d]	−0.48	−1.24		
bpy(no)qH	1.48[f]	0.05[f]	−0.70[f]		

[a] Note: The semiquinone complexes as well as (oo)cat complexes generate cyclic voltammograms with potentials identical with those of their respective quinone form. Solvent = acetonitrile; [TBA(PF_6)] = 0.1 M; [complex] = 1×10^{-3} M. The labels 1 and 2 on the bipyridine potentials refer to reduction of the first and second bipyridine unit. [b] Chemically irreversible, at scan rate 200 mV/s. [c] Peak potential. All data quoted versus SCE. [d] Quasi-reversible at scan rate 200 mV/s (p−p > 100 mV). [e] Data in ref 7 were adjusted to SCE from the internal ferrocenium/ferrocene potential by using a different, less accurate potential. These data assume Fc^+/Fc lies at +0.425 vs SCE. [f] Circumstantially acquired from cyclic voltammogram of $Ru(bpy)_2(no)catH_2^+$. Cyclic voltammogram taken in DCE.

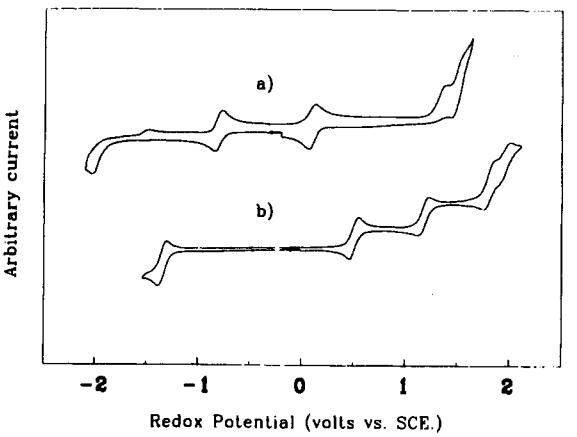

Figure 1. Cyclic voltammograms of the *o*-phenylene ligand complexes: (a) ca. 10^{-3} M bpy(oo)cat in DCE, 0.1 M TBAH, scan rate 200 mV/s, (b) ca. 10^{-3} M bpy(nn)qH_2 in acetonitrile, 0.1 M TBAH, scan rate 200 mV/s.

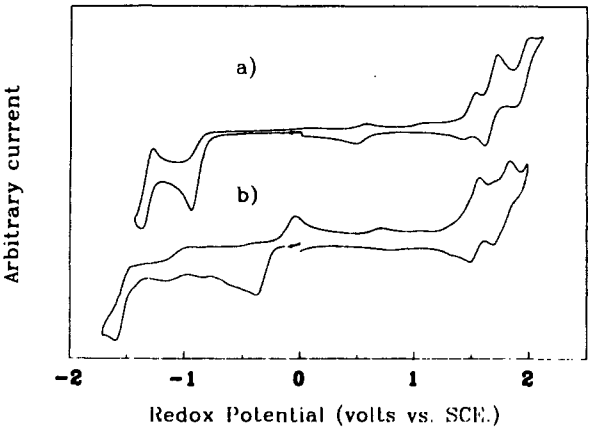

Figure 2. Cyclic voltammograms of catechol complexes: (a) ca. 10^{-3} M bpy(no)$catH_2$ in acetonitrile, 0.1 M TBAH, scan rate 200 mV/s, (b) ca. 10^{-3} M bpy(nn)$catH_4$ in acetonitrile, 0.1 M TBAH, scan rate 200 mV/s.

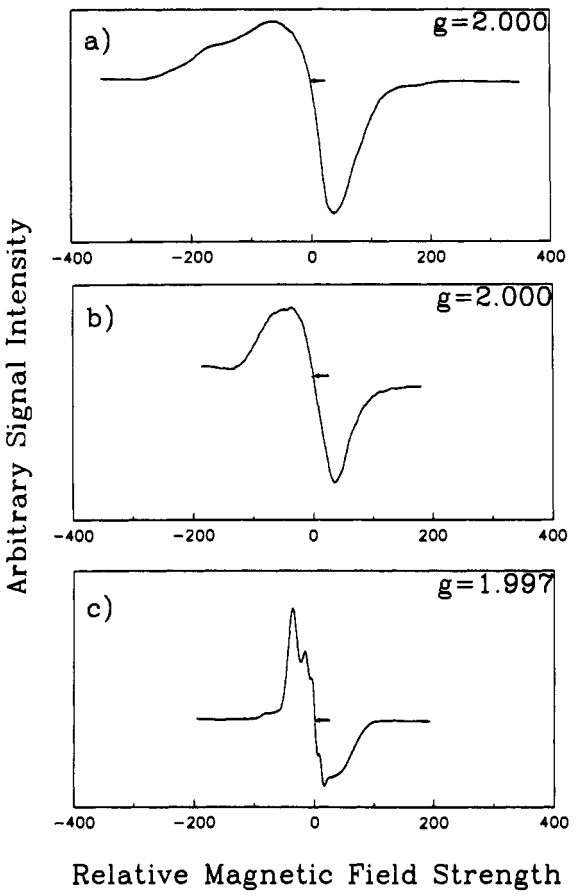

Figure 3. ESR spectra of the semiquinone complexes at 100 K: (a) ca. 10^{-5} M bpy(oo)sq in DCE; (b) ca. 10^{-5} M bpy(no)sqH in DCE generated by the oxidation of bpy(no)catH_2 with benzoyl peroxide; (c) ca. 10^{-5} M bpy(nn)sqH_2 in 2-MeTHF generated by the reduction of bpy(nn)qH_2 with cobaltocene.

Once these protons are lost, then the partially deprotonated species on the electrode display reduction waves on the return scan at potentials coinciding with the ligand redox couples of the bpy(no)qH and bpy(nn)qH_2 complexes. These waves are scan-rate dependent, increasing in size relative to the ruthenium and bipyridine redox couples as the scan rate is increased. They are assigned to reductions of the *o*-phenylene ligand in the bpy(no)qH and bpy(nn)qH_2 species generated during the anodic scan.

Spectroelectrochemistry shows that bpy(no)catH_2 is oxidized to bpy(no)qH prior to the metal oxidation; thus, the metal oxidation that is observed in the cyclic voltammogram of bpy(no)catH_2 actually belongs to bpy(no)qH and is reported as such. New reduction waves observed in the electrochemically generated bpy(no)qH have been assigned to the bpy(no)qH redox couples. A similar situation exists in the bpy(nn) complexes. Here, bpy(nn)catH_4 and bpy(nn)qH_2, which were separately isolated, show, within experimental error, the same Ru(III)/Ru(II) potential. Bulk electrolysis at the *o*-phenylene ligand oxidation wave of bpy(nn)catH_4 similarly produces bpy(nn)sqH_2, as shown spectroscopically, and new reduction waves are observed that have potentials coincident with the ligand redox potentials of the isolated bpy(nn)qH_2. The complexes all contain the ruthenium(II) center with the dioxolene being sequentially oxidized to quinone, but see discussion below. Data are collected in Table I.

ESR Spectroscopy. The ESR spectra of the semiquinone complexes (Figure 3) show signals centered around $g = 2$, indicating the presence of a ligand-centered radical. The successive replacement of *o*-phenylene ligand oxygen atoms with nitrogen results in a slight narrowing of the ESR signal [bpy(oo)sq, δpp (peak to peak separation, between main extrema) = 105 G; bpy(no)sqH, δpp = 82 G; bpy(nn)sqH_2, δpp = 75 G; for conditions see caption to Figure 3], the appearance of nitrogen hyperfine structure, and the decrease of the *g* value below that of a free radical [bpy(oo)sq, $g = 2.000$; bpy(no)sqH, $g = 2.000$; bpy(nn)sqH, $g = 1.997$]. The lowering of the *g* value below that of a free radical is typical of a ligand-centered radical complex containing a ruthenium bis(bipyridine) fragment, where the empty bpy π^* orbitals are of slightly higher energy compared to those of the radical ligand.[39]

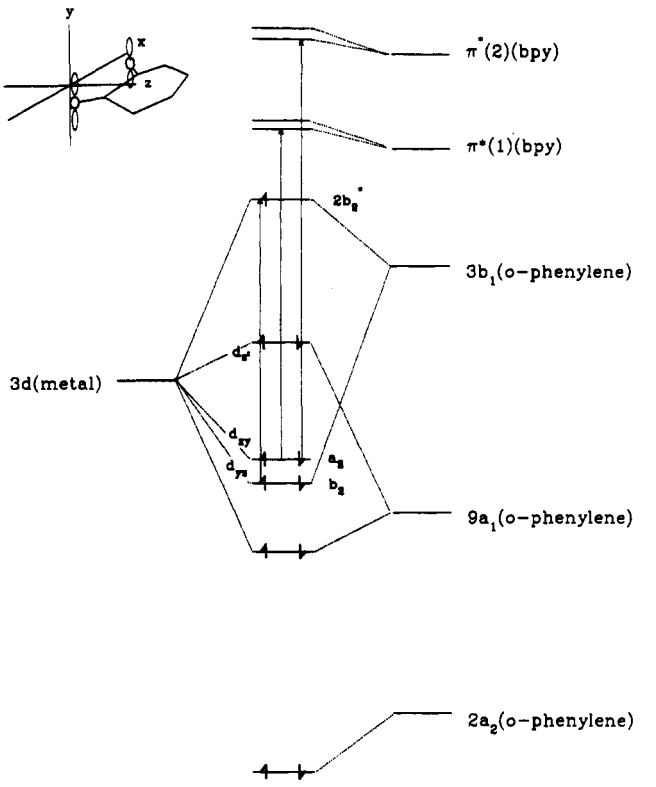

Figure 4. Simplified molecular orbital diagram of the ruthenium bis(bipyridine) semiquinone complexes. The $3b_1$ π^* orbital HOMO contains one electron. The quinone and catechol complexes have one less and one more electron in this orbital, respectively. Vertical solid lines indicate relevant allowed transitions.

Electronic Spectroscopy. The electronic spectra (Table II) of the *o*-phenylene ligand complexes were assigned, as discussed in depth previously,[7] by making comparisons between the bpy complexes and their py analogues and by observing peak shifts caused by both changes in the oxidation state of the complexes and changes in the *o*-phenylene ligand.

The electronic spectra and other characteristics of the *o*-phenylene ligand complexes can be explained by the qualitative molecular orbital (MO) diagram shown in Figure 4. The Gordon and Fenske ligand orbital symmetry labels have been maintained, for discussion of mainly ligand-based orbitals, for ease of comparison with the literature; they apply to the C_{2v} local ligand symmetry;[40] however, it is also acceptable to assign the resulting molecular orbitals in the effective C_{2v} microsymmetry of the central metal. Thus, the metal d_{xy} and d_{yz} orbitals interact with the *o*-phenylene ligand $2a_2$ (π) and $3b_1$ (π^* LUMO) orbitals in weak and strong π interactions, respectively, while the d_{z^2} and d_{xz} orbitals interact with the *o*-phenylene ligand $9a_1$ and $7b_2$ orbitals in weak and strong σ interactions, respectively. The $d_{x^2-y^2}$ orbital remains nonbonding with respect to the *o*-phenylene ligand but is strongly destabilized by σ-bonding with the bipyridine ligands.

The salient features of the π interaction (Figure 4) then are the formation of a pair of orbitals, b_2 and $2b_2^*$ being the bonding and antibonding combinations of the metal d_{yz} and ligand $3b_1$ orbitals (local symmetry label); as will be discussed below, transitions between these two orbitals are a dominant feature of

(39) Ernst, S.; Hänel, P.; Jordanov, J.; Kaim, W.; Kasack, V.; Roth, E. *J. Am. Chem. Soc.* **1989**, *111*, 1733.
(40) Gordon, D. J.; Fenske, R. F. *Inorg. Chem.* **1982**, *21*, 2907, 2916.

Table II. Electronic Spectra of RuN_4L, Where N = Bis(bipyridine)/Tetrapyridine and L = Diimines/Dioxolenes

no.	species	λ_{max}/cm^{-1}	log ϵ (f)[a]	assgnt	solvent
1	bpy(nn)catH_4	21 100	3.73	Ru(II) → π^*(1) bpy	MeCN
		29 700	3.62	Ru(II) → π^*(2) bpy	
		34 200	4.40	π bpy → π^*(1) bpy	
		40 800	4.09	π bpy → π^*(2) bpy	
2	py(nn)catH_4	26 000	4.22	Ru(II) → π^*(1) py	10% HOAc
3	bpy(no)catH_2	15 000 (sh)		$3b_1$ (no)cat → π^*(1) bpy[b]	DCE
		18 900	3.95	Ru(II) → π^*(1) bpy	
		23 650 (sh)		Ru(II) → π^*(1) bpy	
		27 000	3.90	Ru(II) → π^*(2) bpy	
		33 750	4.73	π bpy → π^*(1) bpy	
4	bpy(oo)cat	13 700 (br)	3.64	$3b_1$ (oo)cat → π^*(1) bpy	DCE
		16 200	3.96	Ru(II) → π^*(1) bpy	
		20 850–24 650		$3b_1$ (oo)cat → π^*(2) bpy	
		26 300	4.03	Ru(II) → π^*(2) bpy	
		30 050	4.06	π (oo)cat → π^* (oo)cat	
5	py(oo)cat	19 200 (sh)		$3b_1$ (oo)cat → π^*(1) py	DCE
		21 700	4.15	Ru(II) → π^*(1) py	
		25 400	4.07	Ru(II) → π^*(1) py	
		29 400	3.91	$3b_1$ → π^*(2) py	
6	bpy(oo)catH	18 800	3.88	Ru → π^*(1) bpy	DCE
		27 400	3.95	Ru → π^*(2) bpy	
7	py(oo)catH	25 200	4.21	Ru → π^*(1) py	
8	bpy(nn)sqH_2	10 650	3.02	$2b_2^*$ → π^*(1) LLCT	MeCN
		16 000	4.05 (0.11)	Ru(II) → $3b_1$ (nn)sqH_2	
		18 700 (sh)		Ru(II) → π^*(1) bpy	
		20 150	3.96 (0.10)	Ru(II) → π^*(1) bpy	
		22 000 (sh)		$9a_1$ → π^*(1) bpy LLCT	
		23 000	3.88	$2a_2$ → $3b_1$ intraligand (nn)sq	
		28 650	3.91	Ru(II) → π^*(2) bpy	
9	py(nn)sqH_2	15 150	4.02 (0.10)	Ru(II) → $3b_1$ (nn)sq	DCE
		18 700		py(nn)q impurity	
		25 450	4.16 (0.46)	Ru(II) → π^*(1) bpy	
10	bpy(no)sqH	12 200 (sh)	3.1	$2b_2^*$ → π^*(1) bpy LLCT	DCE
		14 700	4.00 (0.13)	Ru(II) → $3b_1$	
		19 100	3.95 (0.13)	Ru(II) → π^*(1) bpy	
		20 200	3.93	Ru(II) → π^*(1) bpy	
		26 200	3.99	$2a_2$ → $3b_1$ intraligand (no)sq	
		28 550	4.00	Ru(II) → π^*(2) bpy	
11	bpy(oo)sq	11 250	4.29 (0.14)	Ru(II) → $3b_1$ (oo)sq	DCE
		17 250 (sh)		$3b_1$ (oo)sq → π^*(1) bpy	
		19 400		Ru(II) → π^*(1) bpy	
		20 300	3.87 (0.12)	Ru(II) → π^*(1) bpy	
		29 050	4.02	Ru(II) → π^*(2) bpy + $2a_2$ → $3b_1$ intraligand (oo)sq	
12	py(oo)sq	10 600	3.95 (0.11)	Ru(II) → $3b_1$ (oo)sq	DCE
		18 000		$3b_1$ (oo)sq → π^*(1) py	
		27 900	4.12 (0.40)	Ru(II) → π^*(1) py	
		40 950	4.13	π py → π^*(1) py	
13	bpy(nn)qH_2	13 250	2.82		MeCN
		19 400	4.34 (0.26)	Ru(II) → $3b_1$ (nn)qH_2	
		22 450 (sh)	3.89 (0.09)	Ru(II) → π^*(1) bpy	
		30 850 (sh)		Ru(II) → π^*(2) bpy	
		35 600	4.61	π bpy → π^*(1) bpy	
		41 300	3.66	π bpy → π^*(2) bpy	
14	py(nn)qH_2	18 700	4.14 (0.22)	Ru(II) → $3b_1$ (nn)qH_2	DCE
		31 900	4.07 (0.31)	Ru(II) → π^*(1) py	
		34 600 (sh)	4.03	π (nn)qH_2 → π^* (nn)qH_2	
		41 800	4.44	π py → π^*(1) py	
15	bpy(no)qH	17 400	4.10 (0.21)	Ru(II) → $3b_1$ (no)qH	DCE
		20 500	3.88	Ru(II) → $3b_1$ (no)qH	
		23 000		Ru(II) → π^*(1) bpy	
		27 350	3.93	Ru(II) → π^*(2) bpy	
16	bpy(oo)q	15 600	4.12 (0.23)	Ru(II) → $3b_1$ (oo)q	DCE
		33 500 (sh)		$9a_1$ → $3b_1$ intraligand (oo)q	
		25 600	3.88	Ru(II) → π^*(1) bpy	
		27 800	3.88	$2a_2$ → $3b_1$ intraligand (oo)q	
17	py(oo)q	15 600	3.76 (0.32)	Ru(II) → $3b_1$ (oo)q	DCE
		30 000	4.06 (0.47)	Ru(II) → π^*(1) py	

[a] Oscillator strength. [b] $3b_1$ is an approximate label since the (no) ligand is not strictly C_2 in symmetry. There is a weak band in the spectrum of bpy(no)qH, at 20 500 cm^{-1}, which might reasonably have been associated with the Ru → π^*(1) bpy transition. The 20 500-cm^{-1} band is probably the overlap forbidden component of the *o*-phenylene MLCT transition.

the electronic spectra of these species.

The relative arrangement of the bpy and *o*-phenylene ligand-based π^*-MO energies is supported by electrochemical data and by the ligand centeredness of the semiquinone complex ESR signals, which originate from an unpaired electron residing in the semiquinone π^* MO.

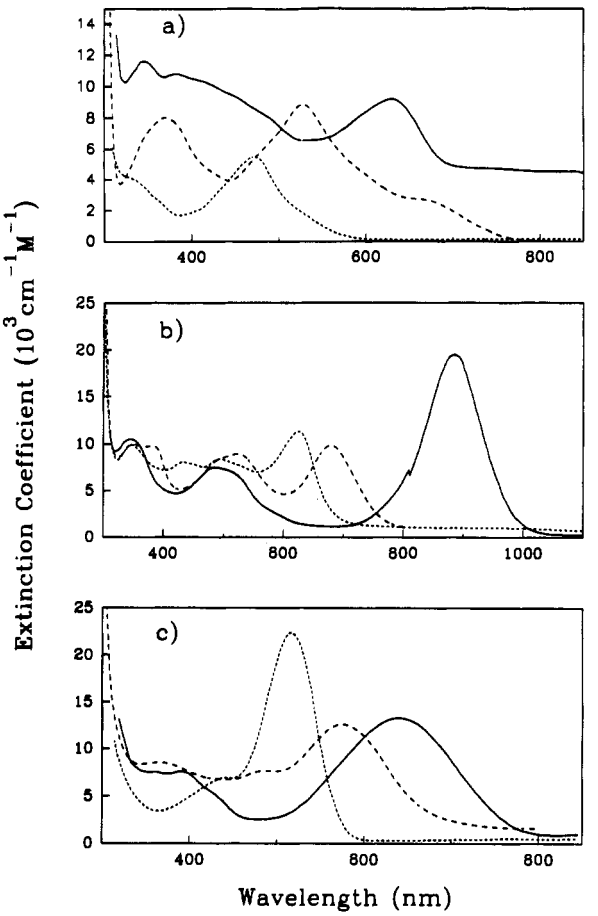

Figure 5. Electronic spectra of ruthenium bis(bipyridine) *o*-phenylene ligand complexes: (a) catechol ligand oxidation state; (b) semiquinone ligand oxidation state; (c) quinone ligand oxidation state. Key: (—) catechol series (oo), DCE; (---) *o*-aminophenol series (no), DCE; (···) *o*-phenylenediamine series (nn), MeCN.

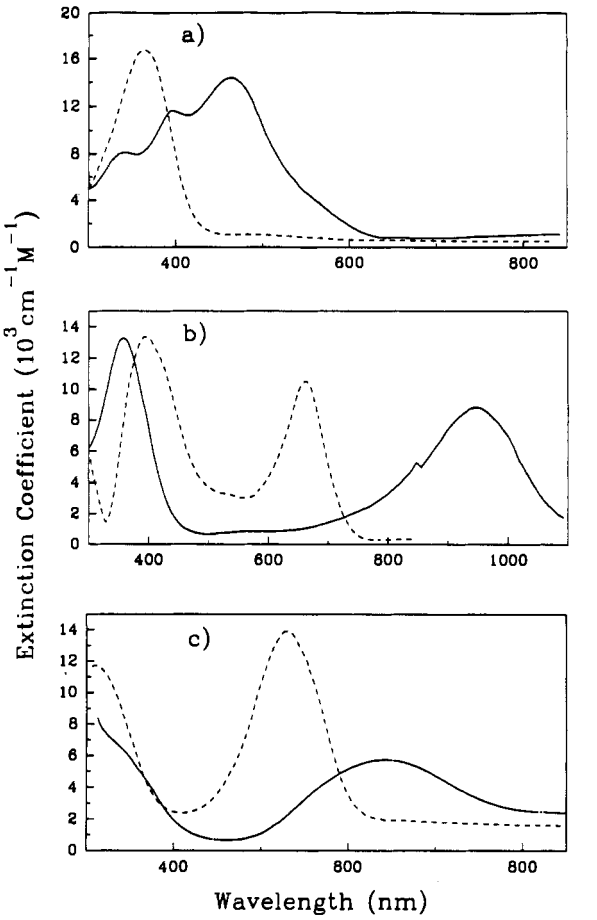

Figure 6. Electronic spectra of ruthenium tetrapyridine *o*-phenylene ligand complexes: (a) catechol ligand oxidation state; (b) semiquinone ligand oxidation state; (c) quinone ligand oxidation state. Key: (—) catechol series (oo), DCE; (---) *o*-phenylenediamine series (nn), DCE.

(a) Catechol Complexes. The catechol complexes are unambiguously ruthenium(II) species comprised of fully reduced *o*-phenylene ligands, which offer no low-lying energy levels to which MLCT transitions can occur. This is also confirmed by the ruthenium $3d_{5/2}$ core photoelectron spectrum (see Experimental Section) of bpy(nn)catH_4, which is consistent with ruthenium(II).[41-48]

All of the intense visible region absorptions must therefore originate from MLCT transitions to either the bpy or py π^* orbitals or from $\pi \rightarrow \pi^*$ intraligand transitions. These latter transitions are high in energy and occur in the UV region.[49] Thus, the bands observed in the visible spectra of the bpy complexes, covering the region from 16 000 to 21 000 cm^{-1} (Figure 5a), are assigned to the Ru $\rightarrow \pi^*(1)$ bpy transitions, while those lying approximately 8500 cm^{-1} higher in energy are assigned to Ru $\rightarrow \pi^*(2)$ bpy transitions (referring respectively to the LUMO and SLUMO orbitals on the bipyridine ligand). The strongest band in the visible spectra of the py complexes (Figure 6a) is assigned to the Ru $\rightarrow$ py $\pi^*(1)$ transition.

The MLCT transitions to bipyridine (or pyridine) shift to higher energies as the number of nitrogen donors on the *o*-phenylene ligand increases (Figure 7); this is a direct consequence of the change in net charge on these ligands, from −2 to 0, respectively, caused by the additional protons on the coordinating nitrogen atoms.

These transitions are relatively broad, due to the ligand field splitting of the metal d-orbital energies and ligand–ligand interaction. While the (oo)cat complexes carry no protons, it is possible to protonate these species in situ by addition of trifluoroacetic acid. This causes a shift to higher energy of the Ru $\rightarrow \pi^*(1)$ bpy transition (Figure 8). Both the protonated pyridine and bipyridine catechol complexes exhibit Ru $\rightarrow$ py/bpy charge-transfer bands at energies that are slightly lower than those of the bpy(no)catH_2 complexes, suggesting that the protonated species are singly protonated, since double protonation should yield a higher charge-transfer energy than in the bpy(no)catH_2 complexes.

The spectra of the (oo)cat and (no)catH complexes are complicated by broad, ill-resolved, interligand charge-transfer (LLCT) bands, which involve transitions from the lone-pair orbitals of the *o*-phenylene ligand oxygen atoms to the π^* orbitals of bpy or py (Table II). Preliminary resonance Raman data for bpy(no)catH_2 support this assignment to a LLCT transition.[50] Such transitions do not occur from nitrogen donor atoms, since these pairs are bound to hydrogen. The transitions are expected to be relatively weak, because of poor overlap, and relatively broad, because of a significant reorganization contribution.

From methods[51] based upon the observed oxidation and reduction potentials of the bpy(oo)cat complex, the $3b_1$ (cat) $\rightarrow$

(41) Weaver, T. R.; Meyer, T. J.; Adeyemi, S. A.; Brown, G. M.; Eckberg, R. P.; Hatfield, W. P.; Johnson, E. C.; Murray, R. W.; Untereker, D. *J. Am. Chem. Soc.* **1975**, *97*, 3039.
(42) Connor, J. A.; Meyer, T. J.; Sullivan, B. P. *Inorg. Chem.* **1979**, *18*, 1388.
(43) Feltham, R. D.; Brant, P. *J. Am. Chem. Soc.* **1982**, *104*, 641.
(44) Srivastava, S. *App. Spectrosc. Rev.* **1986**, *22*, 401.
(45) Geselowitz, D. A.; Kutner, W.; Meyer, T. J. *Inorg. Chem.* **1986**, *25*, 2015.
(46) Brant, P.; Stephenson, T. A. *Inorg. Chem.* **1987**, *26*, 22.
(47) Shepherd, R. E.; Proctor, A.; Henderson, W. W.; Myser, T. K. *Inorg. Chem.* **1987**, *26*, 2440.
(48) Gassman, P. G.; Winter, C. H. *J. Am. Chem. Soc.* **1988**, *110*, 6130.
(49) Bryant, G. M.; Fergusson, J. E.; Powell, H. J. *Aust. J. Chem.* **1971**, *24*, 257.
(50) Stufkens, D. J.; Lever, A. B. P. Unpublished observations.
(51) Dodsworth, E. S.; Lever, A. B. P. *Chem. Phys. Lett.* **1985**, *119*, 61.

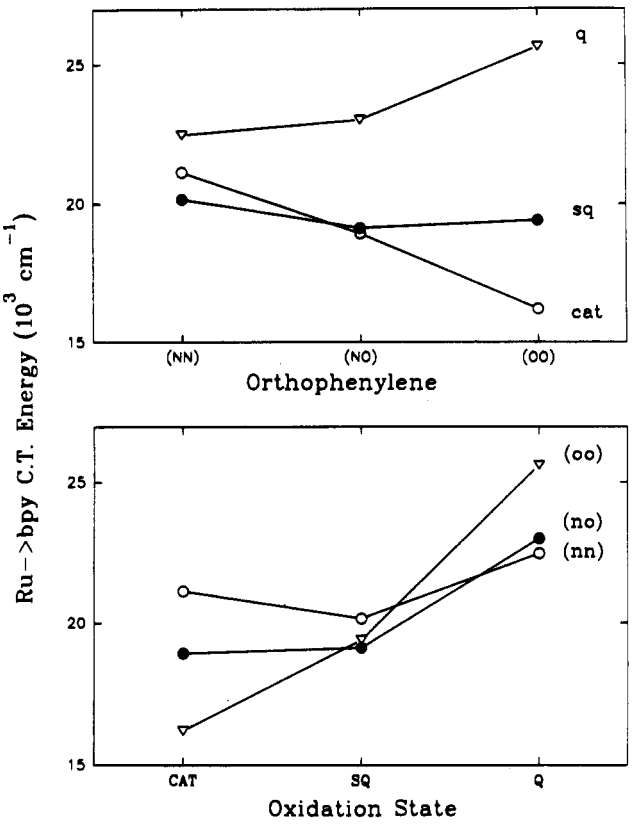

Figure 7. Optical energy shifts of the Ru → $\pi^*(1)$ bpy MLCT as a function of oxygen donor substitution by nitrogen: q = quinone oxidation state; sq = semiquinone oxidation state; cat = catechol oxidation state. This graph also closely approximates, in a relative sense, the variation in Ru(III)/Ru(II) potential as a function of ligand and oxidation state (see text).

$\pi^*(1)$ bpy transition can be calculated to lie at approximately 11 200 cm^{-1} exclusive of reorganization energy, which is then estimated to be about 2500 cm^{-1}. One might have expected the corresponding transition in bpy(no)catH_2 to lie at lower energies, since nitrogen is less electronegative than oxygen. It does not do so because of the protons present on the nitrogen atom. It would lie lower in the deprotonated bpy(no)cat species, which we have not been able to isolate (see Experimental Section).

When the bpy(oo)cat complexes are singly protonated with trifluoroacetic acid in DCE solutions, the LLCT bands vanish and the spectra become strikingly similar to the spectra of the bpy(nn)catH_4 and py(nn)catH_4 complexes (Figure 8). Attempts to doubly protonate bpy(oo)cat led to the decomposition of the complex, while several-fold excess of acid added to py(oo)cat did not further change the spectrum of the monoprotonated species.

Since the catechol ligands are electron rich, and readily oxidizable, one might expect to see LMCT transitions from catechol oxygen electron pairs to the empty d_{xz} and $d_{x^2-y^2}$ orbitals on Ru^{II} (see Figure 4 for coordinate scheme). No evidence for these transitions was seen; they may be expected to contribute to absorption above 30 000 cm^{-1} but will be weak due to overlap constraints.

(b) Semiquinone Complexes. The ESR spectra of these species show that the unpaired electron is located primarily on the semiquinone ligand and therefore that the proper description of these species is ruthenium(II) semiquinone. On the other hand, the analogous osmium (oo) complex[52] has a dramatically different ESR spectrum, characteristic of osmium(III) and therefore an Os^{III}(oo)(cat) electronic structure.

The electronic spectra of the ruthenium(II) semiquinone complexes (Figures 5b and 6b) are dominated by an intense absorption at low energies (log ϵ = 3.9–4.3; E_{op} = 10 500–16 000 cm^{-1}),

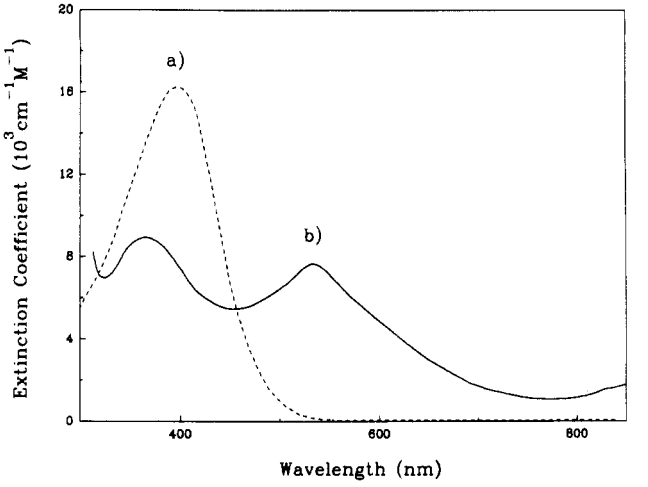

Figure 8. Electronic spectra of protonated catechol complexes: (—) bpy(oo)catH, DCE; (---) py(oo)catH, DCE.

assigned previously to a MLCT to the *o*-phenylene ligand whose half-filled $3b_1$ π^* orbital ($2b_2^*$ in the MO scheme in Figure 4) is now accessible. This transition dramatically shifts to higher energies with the number of nitrogen donor atoms. In a related series of complexes with 4,5-disubstituted 1,2-diiminobenzene ligands, to be reported in detail elsewhere,[53] this transition shifts very significantly to the red with electron-withdrawing substituents, confirming strong MLCT character.

The Ru → bpy charge-transfer bands, which are centered around 20 000 cm^{-1} (Ru → $\pi^*(1)$ bpy) and 29 000 cm^{-1} (Ru → $\pi^*(2)$ bpy), shift little with changes in the number of nitrogen donors in the *o*-phenylene ligand (Figure 7) and are easily distinguished from the Ru → *o*-phenylene ligand (a_2, b_2 → $2b_2^*$) band due to their lower extinction coefficients (log ϵ = 3.6–4.0) and irregular band shapes (Table II).

The spectra of the semiquinone complexes are complicated by both inter- and intraligand transitions whose assignments[54] are tentative (Table II). The $2a_2$ → $3b_1$ intraligand transition, which is centered in the near-UV region in free semiquinone[55] as well as in Zn(II) and Ni(II) complexes,[16] probably accounts for the absorptions near 26 200 and 23 000 cm^{-1} in the bpy(no)sqH and bpy(nn)sqH_2 species, respectively. This absorption is probably obscured by the Ru → $\pi^*(2)$ bpy band in the bpy(oo)sq species.

The energies of the $3b_1$ sq → π^* bpy LLCT bands can be estimated from the electrochemical potentials,[56] as noted above. From data in Table I, this transition, in bpy(oo)sq, is predicted to lie near 18 400 cm^{-1} exclusive of a reorganization contribution. The broad band near 20 000 cm^{-1} likely contains this band. Although py(nn)sqH_2 also appears to exhibit a weak transition around 18 700 cm^{-1}, this is probably due to residual py(nn)qH_2 present from the synthesis of the complex.

There are broad near-infrared absorptions of low intensity in both the bpy(nn)sqH_2 and bpy(no)sqH complexes at 10 650 and 12 200 cm^{-1}, respectively, whose provenance is unknown. They may be spin-forbidden CT bands, $2b_2^*$ → $\pi^*(1)$ bpy transitions, or internal n → π^* sq (Table II).

(c) Quinone Complexes. An X-ray structure of (bpy)(nn)qH_2 shows[23] C=N bond lengths typical of a quinonoid ligand, implying therefore a ruthenium(II) formulation. The Ru $3d_{5/2}$ core photoelectron spectra (see Experimental Section) are in the border region, high but not unacceptable for Ru(II) and low, but possible, for Ru(III).

The quinone complexes exhibit an intense electronic absorption at E_{op} = 15 600–19 400 cm^{-1} (log ϵ = 3.76–4.34), which shifts to higher energy as the number of nitrogen donors on the *o*-phenylene

(52) Haga, M.-A.; Isobe, K.; Boone, S. R.; Pierpont, C. G. *Inorg. Chem.* **1990**, *29*, 3795.
(53) Masui, H.; Lever, A. B. P. Manuscript in preparation.
(54) Dodsworth, E. S.; Lever, A. B. P. *Chem. Phys. Lett.* **1990**, *172*, 151.
(55) Stallings, M. D.; Morrison, M. M.; Sawyer, D. T. *Inorg. Chem.* **1981**, *20*, 2655.
(56) Dodsworth, E. S.; Lever, A. B. P. *Chem. Phys. Lett.* **1986**, *124*, 152.

ligand increases (Figures 5c and 6c and Table II). This absorption has also been previously assigned to a Ru → $3b_1$ ($b_2 \rightarrow 2b_2^*$) MLCT transition.[7]

The transitions are broader than the corresponding Ru → sq transitions (vide infra). In the aforementioned study of complexes with 4,5-disubstituted 1,2-diiminobenzene ligands,[53] this transition, in the quinone complexes, does not shift regularly with electron-withdrawing substituents, and the magnitude of the shift is half that observed for the semiquinone species discussed above. The small shifts are, however, more reconcilable with an LMCT transition than with an MLCT transition. The corresponding Ru → quinone transition in $Ru(NH_3)_4$(oo)q occurs at[57] 19 500 cm^{-1}, significantly higher in energy than observed in the bipyridine analogue. Since the $Ru(NH_3)_4$ fragment is certainly easier to oxidize than the $Ru(bpy)_2$ fragment, this observation would again be consistent with an LMCT transition rather than an MLCT transition.

The Ru → quinone transitions in $[Ru(bpy)_2RBQ]^{2+}$ occur[7] at 14 950 cm^{-1} with RBQ = 3,5-di-*tert*-butyl-1,2-benzenequinone and at 15 650 cm^{-1} with RBQ = 3,4,5,6-tetrachloro-1,2-benzenequinone, compared with 15 600 cm^{-1} for bpy(oo)q. The lack of a shift upon chlorine substitution suggests little charge-transfer character, while the blue shift with the more electron-donating *tert*-butyl-substituted species is again more reconcilable with a LMCT than MLCT transition. Resonance Raman data, exciting into the Ru → quinone ($b_2 \rightarrow 2b_2^*$) transition of bpy(oo)q, revealed vibrational enhancements consistent with little charge-transfer character.[8] These observations bring into question whether this transition should, in fact, be represented Ru → quinone or rather semiquinone → Ru. We return below to further consideration of these observations and, to avoid misrepresentation, refer henceforth to this transition as Ru/quinone.

The Ru → π^*(1) bpy band appears at higher energies and with lower intensity than the Ru/quinone transition. This Ru → π^*(1) bpy band shifts slightly to lower energies with replacement of the oxygen atoms of the *o*-phenylene ligand by nitrogen (Figure 7). In contrast to the behavior of the catechols (vide supra) it is now the more electron-rich (nn) species, in these neutral quinones, placing charge onto the metal atom, which shifts the Ru → π^* bpy transition to lower energy. An internal *o*-phenylene ligand transition may occur at similar energies.

Energy Matching, Ruthenium-Ligand Orbital Mixing, and Reorganization Energies. The degree of orbital mixing, specifically in the b_2 and $2b_2^*$ orbitals, will depend upon the matching of orbital and metal energies and the extent of (symmetry-permitted) overlap.

An experimental measure of the mixing can be obtained through analysis of the reorganization energies involved in the $b_2 \rightarrow 2b_2^*$ transitions. A transition from a metal-localized orbital to a ligand-localized orbital should exhibit significant reorganization energy, with strong charge-transfer character, especially as the bond distances in these *o*-phenylene ligands are very dependent upon their net oxidation state. A small reorganization energy signals a transition between largely mixed metal–ligand orbitals[58] and, in our systems, with little charge-transfer character.

Reorganization energies may be estimated, in a relative sense, from the half-bandwidths of the relevant transitions.[59] However, of the two possible observable transitions, one, $b_2 \rightarrow 2b_2^*$, is strongly allowed and the other $a_2 \rightarrow 2b_2^*$ is allowed but with poor overlap;[60,61] both may occur within the same band envelope. The $a_1 \rightarrow 2b_2^*$ transition would vanish through overlap orthogonality. The bandwidth may, therefore, reflect the degree of splitting between the b_2 and a_2 metal orbitals. The extent of such splitting will depend upon the true symmetry and on differences between the π interactions of the bipyridine and *o*-phenylene ligands.

Table III. Transition Bandwidths (cm^{-1})

Bipyridine Complexes			
Ru → (nn)sqH_2	2100	Ru → (nn)qH_2	2500
Ru → (no)sqH	2200	Ru → (no)qH	3800
Ru → (oo)sq	1400	Ru → (oo)q	3950[a]
Pyridine Complexes			
Ru → (nn)sqH_2	2050	Ru → (nn)qH_2	3450
Ru → (oo)sq	2400	Ru → (oo)q	5300

[a] Half-bandwidth data for Ru(II) (oo)q derivatives were in error (too small) by a factor of 2 in the previous paper.[7]

The bpy (nn) and py (nn) species have a RuN_6 pseudooctahedral symmetry, and the (oo) species, while technically C_2, has a pseudo-D_{4h} splitting pattern; both these point groups, if they rigorously applied, would make the a_2 and b_2 orbitals degenerate. Thus, both these species are of relatively high symmetry. On the other hand, the (no) species can only possess C_1 symmetry. On this basis, the splitting of the CT bands should be greatest in the (no) species, and this is seen to be the case (Table III).

Specifically for the (nn) and (oo) species, the relative reorganization energies may be compared directly by considering the half-bandwidths of the transitions in the semiquinone and quinone species (Table III).

For a given *o*-phenylene ligand, the Ru → sq MLCT transitions are narrower than the Ru/quinone transitions. For the quinone oxidation state, the Ru/quinone band is narrowest in the species bpy(nn)qH_2, and for the semiquinone oxidation state, the Ru → $3b_1$ ($b_2 \rightarrow 2b_2$) semiquinone transition in bpy(oo)sq is slightly narrower than in bpy(nn)sqH_2 but there is little difference (Table III).

The observation that the bpy(nn)qH_2 complex Ru/quinone transition has a narrower band than that in the bpy(oo)q complex, yet lies at higher energy, is very unusual. Generally speaking bands of similar origin become broader as they shift to higher energies.[59,61]

(a) Electronic Structure of the Semiquinone Species. Thus, in view of the very narrow Ru → sq ($b_2 \rightarrow 2b_2^*$) transitions, the degree of mixing between metal d_{yz} and semiquinone ligand $3b_1$ (see Figure 4) (in b_2 and $2b_2^*$) is considerable and a little more important in the (oo) series than in the (nn) series because of better energy matching. Overlap terms may be comparable for the three negatively charged semiquinone ligands.

The resulting $2b_2^*$ LUMO, containing the unpaired electron, has greater ligand character in the (nn) series than in the (oo) series, fully consistent with the observed electron spin resonance data.

The oscillator strengths of the Ru → sq MLCT band are quite large (Table II), slightly more so for the (oo)sq species than for the (nn)sqH_2 species. The combination of narrower band and higher oscillator strength is particularly significant. Since intensity arises from $\langle L|r|L\rangle$ matrix elements,[61,62] such an observation also indicates a greater degree of mixing for the bpy(oo)sq species relative to bpy(nn)sqH_2.

(b) Electronic Structure of the Quinone Species. In the quinone oxidation state, we propose that such metal/ligand mixing, in the b_2 and $2b_2^*$ orbitals, is significantly better for the (nn) series than for the (oo) series and greater than in the semiquinone series. Overlap, and hence mixing, will also be better in the (nn) series than in the (oo) series because of the greater electron richness of the former as indicated by the shift in the Ru → π^* bpy transition, noted above (Figure 7).

This proposal leads to the conclusion that the b_2 orbital will have more ligand character in the (nn) series than in the (oo) series, and therefore the, now empty, antibonding combination (LUMO) will have more metal character in the (nn) series than in the (oo) series.

(57) Pell, S. D.; Salmonsen, R. B.; Abelleira, A.; Clarke, M. J. *Inorg. Chem.* **1984**, *23*, 385.
(58) The converse is not necessarily true; i.e., transition between highly mixed states do not always lead to narrow transitions.
(59) Renk, I. W.; Dieck, t. D. *Chem. Ber.* **1972**, *105*, 1403.
(60) Balk, R. W.; Stufkens, D. J.; Oskam, A. *Inorg. Chim. Acta* **1979**, *34*, 267.
(61) Lever, A. B. P. *Inorganic Electronic Spectroscopy*, 2nd ed.; Elsevier: Amsterdam, 1984.
(62) Desjardins, S. R.; Penfield, K. W.; Cohen, Su. L.; Musselman, R. L.; Solomon, E. I. *J. Am. Chem. Soc.* **1983**, *105*, 4590.

This supposition explains the very narrow Ru/quinone transition in bpy(nn)qH_2 relative to that in bpy(oo)q (and similar but less dramatic observation in the pyridine analogues). There is greater mixing of the orbitals and less charge transfer character of the transition in the (nn) series (cf. resonance Raman data cited above). This also explains why these transitions, to the extent that they do have charge-transfer character, are ill-behaved, demonstrating characteristics of both MLCT and LMCT transitions. The shift to higher energy for the Ru/Q transition in these quinones relative to the corresponding band in the semiquinones arises from the strong overlap stabilization. This problem is addressed in more detail elsewhere.[53]

Note that the strong interaction proposed between the d_{yz} metal orbital and ligand $3b_1$ orbital is equivalent to describing a π-back-bonding interaction between the metal and the quinone ligand. This is supported by an X-ray study[23] of $[Ru^{II}(bpy)_2(nn)qH_2](PF_6)_2$, demonstrating that the Ru–N(diimine) bond (2.02 Å) was substantially shorter than the Ru–N(bipyridine) bond (2.08 Å), which fact was attributed to significant π back-donation to the diimine ligand.

In parallel with the observation reported above for Ru(oo)sq, the oscillator strength for the Ru/quinone transition is at a maximum for the bpy(nn)qH_2 species, consistent with greater mixing therein. The extra mixing, and presumable stabilization of the quinonediimine species may also explain why many (quinonediimine)ruthenium complexes have been reported in the literature but few, if any, (quinone)ruthenium(II) species have been isolated.

Although these complexes are described here as ruthenium(II) quinone derivatives, it is pertinent, in the light of the above discussion, to ask whether they should indeed be so described. A strong interaction between metal d_{yz} and ligand $3b_1$ orbitals, with the b_2 orbital being more ligandlike and containing two electrons, leads to the formal description $[Ru^{III}(bpy)_2sq]^{2+}$, if weighted electron populations are summed (assuming the b_2 orbital to be 50:50 M/L). Such a discussion of apparent oxidation state is reminiscent of early work by tom Dieck[59,63] on molybdenum phosphine carbonyl species, which behave in an analogous fashion, and of similar discussions by Meyer.[37,42,64] The report is also relevant to earlier studies of the effect of metal–ligand mixing on charge-transfer energies and effective oxidation states by Taube,[65,66] Creutz,[67] and Kaim.[68]

Certainly one may suppose that there is such a Ru^{III} contribution to the description in a valence bond sense, a contribution that is, indeed, consistent with the PES data (Experimental Section).[42-48]

However the X-ray data (quoted above) are appropriate for Ru^{II}, and the Ru → bpy transitions are typical of ruthenium(II) bipyridine species. The observed Ru → $\pi^*(1)$ bpy transition is consistent[56] with the electrochemical potentials as assigned.

In summary, these quinone complexes are considered to be better described by the Ru(II) description rather than the Ru(III) description; i.e., the b_2 orbital is still centered more on the metal than on the ligand.

The osmium complex corresponding with (bpy)(oo)q has electronic spectra interpreted[52] in terms of $[Os^{III}(bpy)_2(DTBSq)]^{2+}$. Thus, the trivalent character is much better expressed in the osmium series, as also observed, for example, in the species $[M(NH_3)_5(N\text{-methylpyraziniumyl})]^{3+}$, M = Ru, Os.[67]

Conclusions

Our studies have provided information concerning the variation in orbital mixing and metal–ligand bonding as a function of ligand donor in these noninnocent systems. There is extensive orbital overlap in many of these complexes leading to no clear distinction between one oxidation state and another, though ruthenium(II) is the best overall description.

Current complementary studies include X-ray structural analyses of some of these species to provide structural data relating to ground state structure, resonance Raman studies to probe the vibrational coupling in the CT and intraligand transitions, and molecular orbital studies to obtain greater insight into the mixing processes involved.

Acknowledgment. We are indebted to the Natural Sciences and Engineering Research Council (Ottawa) and the Office of Naval Research (Washington, D.C.) for financial support. We also thank Dr. Elaine Dodsworth for useful discussion and Johnson Matthey Inc. for the loan of ruthenium trichloride.

(63) tom Dieck, H.; Renk, I. W. *Angew. Chem. Int. Ed. Engl.* **1970**, *9*, 793; tom Dieck, H.; Renk, I. W. *Chem. Ber.* **1971**, *104*, 110.
(64) Sullivan, B. P.; Salmon, D. J.; Meyer, T. J. *Inorg. Chem.* **1978**, *17*, 3334.
(65) Magnuson, R. H.; Taube, H. *J. Am. Chem. Soc.* **1975**, *97*, 5129.
(66) Wishart, J. F.; Bino, A.; Taube, H. *Inorg. Chem.* **1986**, *25*, 3318.
(67) Creutz, C.; Chou, M. H. *Inorg. Chem.* **1987**, *26*, 2995.
(68) Kaim, W.; Gross, R. *Comments Inorg. Chem.* **1988**, *7*, 269.